Lattice model of the early stages of the electrification of a cloud

C. Nicolis
Institut Royal Météorologique de Belgique, Avenue Circulaire 3, 1180 Brussels, Belgium

G. Nicolis
Center for Nonlinear Phenomena and Complex Systems, Université Libre de Bruxelles, Code Postal 231, Boulevard du Triomphe, 1050 Brussels, Belgium

John J. Kozak
Department of Chemistry, Iowa State University, Ames, Iowa 50011, USA

(Received 18 March 2002; revised manuscript received 15 October 2002; published 9 June 2003)

The early stages of the microphysics of the electrification process within a cloud are considered using a two-dimensional lattice model. Using insights generated from Monte Carlo simulations and the theory of finite Markov processes, the mean walk length statistics of the particles, the instantaneous electric potential and electric field profiles, the time evolution of electrostatic energy and their dependence on system size are studied. Some unexpected features of the kinetics of electrification and of the statistics of crossings of the threshold for an electric discharge to occur are brought out.

DOI: 10.1103/PhysRevE.67.061104 PACS number(s): 05.40.−a, 05.10.Ln, 51.50.+v

I. INTRODUCTION

Transient electric discharges occurring within clouds or from cloud to ground rank among the most intriguing natural phenomena. In addition to their fundamental scientific interest they interfere with processes of industrial, economic, and societal concern and, contrary to common belief, they are far from exceptional events [1].

The gross features of the electrification and discharge processes can be summarized as follows. Strongly convective clouds generated by the thermal instability of humid air develop rapidly in thunderstorm cells. During this dynamical development, strong updrafts carry up ice crystals, droplets, and graupels. These particles become charged and are subsequently separated by their differential vertical motions inside the cloud. This process induces an electrification of the storm cell resulting in a multipole structure with positive charges at the cloud base. When the amplitude of the electrical field attains a sufficiently high value inside the cloud, the first cloud-to-cloud lightnings occur. The maximum lightning activity takes place when the vertical development of the storm is optimal. This is the mature stage of the storm cell. At that time, cloud-to-ground lightnings appear and may cause considerable damage at the ground level.

Several theories have been developed advancing different mechanisms for the microphysics of the charging process [2,3].

(i) The convective theory in which ions generated in the atmospheric boundary layer are convectively trapped into the cloud and induce a charged layer on its boundaries.

(ii) The noninductive theory which postulates that the particles are charged by collisions and separated by updraft and by the gravitational force. The polarity of charge transfer depends, in this case, on the ambient temperature and water content. In particular, there is a charge reversal temperature (at about $-10\,^{\circ}\mathrm{C}$) above which collisions between large graupels and smaller ice crystals result in, respectively, positively and negatively charged heavy and light particles.

(iii) The inductive mechanism which postulates that the charging process is associated with the polarization of drops due to the external electrical field. The opposite charges are subsequently separated by collisions and differential motion as in (ii).

All these mechanisms are believed to contribute to cloud electrification, but their respective roles are still an open question.

The present work is devoted to the early stages of the above charging process. We focus on the noninductive (collisional) mechanism and implement this mechanism on a vertical section of a cloud, assimilated to a square-planar lattice in a thermal environment above the aforementioned charge reversal temperature in which the reactants perform a diffusive motion that will be assimilated in our lattice model as a random walk. Our purpose is to analyze the interplay between kinetics, spatial extent, electrostatic, and gravitational forces in the efficiency of the reactive collision process giving rise to positive and negative charges. In particular, the kinetics of the charge separation process and of the buildup of electric fields above a prescribed threshold will be determined with emphasis on the dependence of the characteristic times on the size and on the boundary conditions. Such characteristic times constitute an important piece of information for the purposes of prediction that, as well known, is especially elusive as far as the timing and localization of an electric discharge are concerned [4].

The general setting is laid down in Sec. II. Section III is devoted to the computation of the characteristic times, measured as the mean walk length $\langle n \rangle$ performed by the particles prior to the termination of the process. The dynamics of the electrification is considered in Sec. IV. The main conclusions are summarized in Sec. V.

II. FORMULATION

Consider a thermodynamically open system involving heavy (H) and light (L) particles, the former being essentially

 ©2003 The American Physical Society

the aggregates of the latter. Particles belonging to these two species can perform a random walk on a square-planar lattice or undergo reactive collisions according to the scheme

$$H^0 + L^0 \rightleftarrows H^+ + L^-, \tag{1}$$

where the superscripts $\pm$, 0 indicate, respectively, positively charged, negatively charged, and electrically neutral forms of H and L. The random walk performed by the heavy species is biased by the effect of gravity, whereas for the light particles it is assumed that gravity is canceled by updraft arising from advection.

Before we undertake the analysis of the above defined dynamics on the lattice it is desirable to establish some connection between the lattice spacing Δr and the particle hopping time Δt on the one side, and the scales involved in typical cloud conditions on the other. As well known, the relevant transfer mechanism is here eddy (turbulent) diffusion rather than molecular diffusion. A typical value of the associated eddy diffusivity coefficient is [5,6] $\kappa_t \approx 10\ \mathrm{m}^2\ \mathrm{s}^{-1}$. It follows that Δr and Δt must satisfy the relation

$$\frac{\Delta r^2}{2\Delta t} = \kappa_t \approx 10.$$

On the other hand, Δr must clearly be of the order of or less than the size, ℓ, of a typical eddy. It is known [7] that much of the energy in turbulent cloud motions is contained in eddies or irregularities smaller than 100 m. Combining this with Richardson's empirical formula for turbulent particle diffusion [6] $\kappa_t = 0.2 l^{4/3}$ we arrive at l values of 10 m or so. Choosing $\Delta r = 10$ m we then obtain from the relation linking Δr to Δt the estimate $\Delta t = 5$ s. The life cycle of a thunder cloud is of about 60 min, i.e., about 700 time units Δt. This places on the mean walk length $\langle n \rangle$ previously defined the upper bound of 700, since the process described by Eq. (1) must be completed within the cloud life cycle.

We now come back to the analysis of our lattice model. To have a well posed problem we need to specify the boundary conditions. As there are no constraints acting along the horizontal direction we choose periodic boundary conditions for this direction. On the other hand, when hitting the lower boundary the particles are subjected to the following conditions: (1) no flux (confining) boundary conditions for L, (2) exit boundary conditions [the particle leaves the system, scenario $(H1)$], or sticky boundary conditions [the particle remains confined in the boundary, scenario $(H2)$] for H with, in the latter case, H being left or not the possibility to perform a random walk in the horizontal direction. Conversely, the following conditions are stipulated in the upper boundary: (1) no flux (confining) boundary conditions for H, (2) exit boundary conditions [scenario $(L1)$] or sticky boundary conditions [scenario $(L2)$] for L with, again, the choice to remain frozen or to perform a random walk in the horizontal direction.

The present work is limited to the case where only two neutral particles of different mass or two charged particles of opposite charge are initially present in the lattice. The process described above will then be terminated when (a), in the scenario $(H1L1)$, H or L reach for the first time the lower or the upper boundary, respectively, or (b), in the scenario $(H2L2)$, when H and L eventually both reach, in any order, the lower and the upper boundary, respectively.

We now specify the rules governing particle interactions and particle collisions. Following recent work by the present authors [8,9], we stipulate that H and L interact via hard core repulsion prohibiting particle crossing and the simultaneous occupation of a given site by more than one particle. A head-on collision where one particle of H^0 and one particle of L^0 type tend to occupy the same position or to cross is considered to be a reactive collision configuration [forward step of Eq. (1)]. It results in the conversion of H^0, L^0 into H^+, L^-, respectively, and the particles are reset thereafter to their previous positions. Conversely, a head-on collision of H^+ and L^- will lead to the replacement by H^0 and L^0 and the subsequent resetting. There is, however, a subtlety in this latter case, since it now seems reasonable to introduce a ''Coulomb bias'' favoring the occurrence of reactive H^+-L^- collisions when the distance between the species is small. In principle, this bias and the one associated with the effect of gravity on the random walk of H are to be described by suitable Boltzmann factors. In practice, in what follows it will be expressed through a fixed enhancement of the transition probability of the relevant step over the other steps, being understood that care is taken to ensure that such conditions as conservation of total probability are satisfied. In particular, in the presence of gravitational bias the downward transition probability will be taken three times larger than the upward one. As for the Coulomb bias in some of the cases it will be taken in its extreme form whereby charged particles in nearest-neighbor positions will react with probability 1.

Despite its apparent simplicity the problem defined by relation (1), the boundary conditions and the collisional rules, is not solvable in a closed form, not even in its mean-field version which already involves four coupled nonlinear reaction-diffusion equations. In the following sections it will be studied by Monte Carlo simulation techniques. Some analytic insight will also be obtained using the theory of finite Markov processes.

In the Monte Carlo simulation, a large number of realizations (typically 10^5) is carried out, covering all possible distinguishable initial configurations. In each realization the allowed transitions are determined following the collision rules and the usual prescriptions of the random walk. The process is terminated when the conditions specified earlier in the present section are satisfied.

Coming to the application of the theory of finite Markov processes, we first briefly review the case of a single diffusing particle and a stationary trap placed at lattice site $i=1$. The probability of the survival (without absorption) of the particle after n time steps starting from any initial site i satisfies the discrete version of the backward Kolmogorov equation. As a consequence of the linearity of this equation, the moments of the survival time until absorption satisfy a system of inhomogeneous, linear, simultaneous equations. Let $T_{i,q}^{(n)}$ (where $q=0, 1, \ldots$) denote the qth moment of the

TABLE I. The Markovian and the Monte Carlo results on mean time prior to termination for a 3×3 and a 5×5 lattice.

		Scenario ($H1L1$) Gravity|Coulomb bias				Scenario ($H2L2$) Gravity and Coulomb bias	
		No|No	No|Yes	Yes|No	Yes|Yes	*H, L* immobile on boundaries	*H, L* mobile on boundaries
3×3 lattice	Markov	10.394	11.949	5.914	7.051	21.688	
	Monte Carlo	10.351	11.938	5.918	7.090	22.200	27.046
5×5 lattice	Markov	21.740	22.915	9.374	10.238	50.592	
	Monte Carlo	21.857	22.803	9.321	10.200	47.790	52.009

survival time (the time to trapping) for a walk originating at site i on a given lattice of size N. Thus, $T_{i,q}^{(n)}$ is also the qth moment of the walk length for a random walk starting at i. By definition $T_{1,q}^{(n)}=0$. For $2<i<N$ we have, recalling that the time step has been set equal to unity,

$$-\Delta_{ij}T_{j,q+1}^{(n)}=(q+1)T_{i,q}^{(n)}, \tag{2}$$

where a summation over the repeated index j is implied, and Δ_{ij} stands for the discrete Laplacian

$$\Delta_{ij}=\frac{1}{\nu_i}\delta_{\langle ij\rangle}^{\mathrm{kr}}-\delta_{ij}^{\mathrm{kr}}. \tag{3}$$

Here, ν_i is the coordination number of site i, $\delta_{ij}^{\mathrm{kr}}$ is the Kronecker delta, and $\langle ij\rangle$ indicates that j is a nearest neighbor of i. The set of equations satisfied by the first moments or mean walk lengths $T_{i,l}^{(n)}$ is obtained by setting $q=0$ in Eq. (2). The quantity $T_{i,o}^{(n)}$ is the zeroth moment of the distribution of the time of first passage to the trap from the origin i, and is equal to unity since absorption at the trap is a sure event for every starting point i. As we shall be concerned throughout with just the set of first moments $T_{i,q}^{(n)}$, we drop the index corresponding to q henceforth and write $T_i^{(n)}$ for this quantity. We therefore have

$$-\Delta_{ij}T_j^{(n)}=1. \tag{4}$$

We seek the mean walk length $T^{(n)}$, which is the average of $T_i^{(n)}$ over starting sites i distributed uniformly over all sites of the lattice other than the trap site $i=1$. This is given by

$$T^{(n)}=\frac{1}{(N-1)}\sum_{i=2}^{N}T_i^{(n)}=\frac{1}{(N-1)}\sum_{i=2}^{N}\sum_{j=2}^{N}(-\Delta^{-1})_{ij}, \tag{5}$$

where use has been made of Eq. (4) in writing the second equality. We note that Δ is a nonsingular matrix.

The generalization of this standard approach to the case of two (or more) simultaneously diffusing particles as in relation (1) is to classify all initial configurations of the particles on a given lattice and to document all concerted motions corresponding to each such configuration into symmetry-distinct states [10]. That is, instead of following the site-to-site transitions of a single particle diffusing on a lattice, one now documents the evolution of (all) joint configurations of two (or more) particles. This being done, the formal apparatus of the backward Kolmogorov equation can be implemented directly, and numerically exact values of the mean lifetime of a reaction pair on a given lattice can be calculated although, contrary to the one walker plus trap case, no general closed form expressions can be derived. The first step in this procedure is to specify the possible two-particle configurations on the lattice under study. For example, on the 3×3 square-planar lattice, there are, in principle, 72 joint configurations (states). For each joint configuration, there are, corresponding to a given displacement of the first particle, four possible displacements of the second particle, a total of 16 new configurations into which a given configuration can evolve. Thus, the Markovian transition probability matrix for the forward reaction in Eq. (1) has 72×16 nonempty entries. Similarly, for two particles undergoing simultaneous displacements on a 5×5 square-planar lattice, there are 600 possible joint configurations, and 600×16 entries in the transition probability matrix.

The problem under study involves a charge transfer forward step and a neutralization reaction for the reverse step. To deal with this complexity, a second manifold of possible transitions, corresponding to the reverse reaction above, was considered explicitly. This second manifold also has 72×16 possible transitions for the 3×3 lattice and 600×16 possible transitions on the 5×5 lattice. Transitions from the first manifold (the forward reaction) to the second manifold (the reverse reaction), and vice versa, were specified to occur upon collision of the respective reactants. Then, using the Markovian theory outlined above, the mean number of displacements of the reactants before the termination of the process (effectively, the mean lifetime of the diffusion-reaction event) was determined directly.

To complete the technical specification of the Markov problem, gravity was introduced by biasing the motion of the heavy particle (only) in its vertical displacements. Coulombic interactions between the two particles in the ''backward''

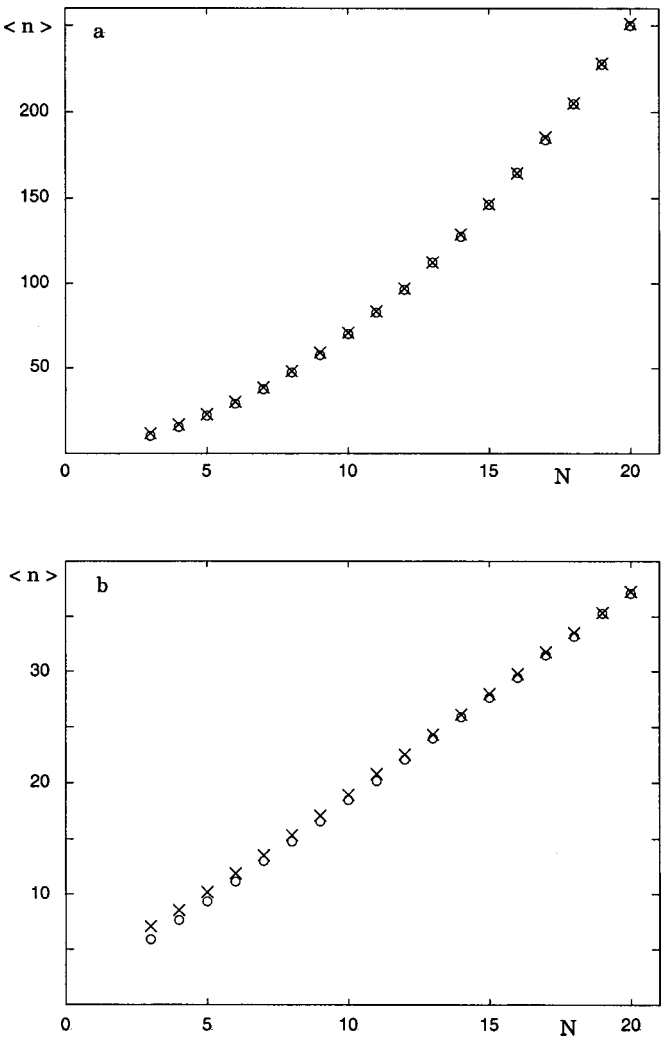

FIG. 1. Mean walk length vs lattice size in the case of the scenario (*H*1*L*1) in the presence of zero (a) and finite (b) gravitational bias. Empty circles stand for no Coulomb bias and crosses for extreme Coulomb bias whenever particles are charged. Averaging is performed over 10^5 realizations and the initial positions (nonoverlapping) of the particles on the lattice as well as their polarity are chosen randomly. Here and in the following figures the quantities plotted are dimensionless.

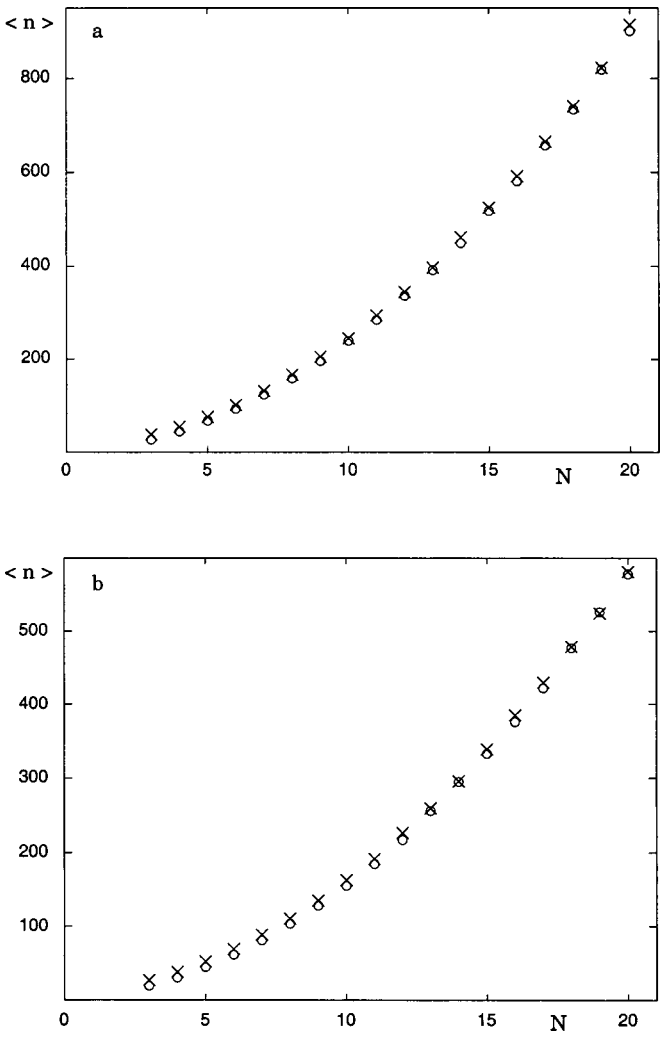

FIG. 2. As in Fig. 1 but in the case of the scenario (*H*2*L*2).

manifold were taken into account by assigning a probability that when the two (charged) particles were adjacent to each other, neutralization occurred in the very next step.

Finally, we note that the imposition of periodic boundary conditions on the vertical boundaries of the cell allows some simplification in the problem, by collapsing the number of joint configurations of the two particles into a subset of symmetry-distinct configurations. In the 5×5 lattice, for example, the total number of symmetry-distinct configurations that needed to be considered dropped to 78 (for each manifold) when periodicity on the vertical boundaries was taken into account.

III. WALK LENGTH STATISTICS

Table I summarizes the Markovian and the Monte Carlo results on the mean time prior to termination for a 3×3 and a 5×5 lattice under the various conditions defined in the preceding section. Both exit and sticky boundary conditions are considered. As noted previously, the gravity bias when present, is expressed by an enhanced downward transition probability of $\frac{3}{8}$. The Coulomb bias, when present, is here taken in its most extreme version in which if the two particles initially occupy adjacent or next to adjacent positions, reaction will occur with probability 1.

As seen from the table, the agreement between the Markov and the Monte Carlo results is excellent throughout, except in one of the situations pertaining to sticky boundary conditions where a difference of about 5% is found. Generally speaking, the gravity bias tends to accelerate the process drastically. The effect of the Coulomb bias goes in the opposite direction, but is less drastic that the gravitational one.

The Monte Carlo simulations have also been extended to lattices of sizes up to 20×20, for which the Markovian approach becomes impracticable. In view of the discussion on space scales at the beginning of Sec. II, such sizes correspond to a linear dimension of up to a few hundred meters. They allow us to capture some essential parts of the dynamics, since a typical vertical extent of a single thunder cloud is

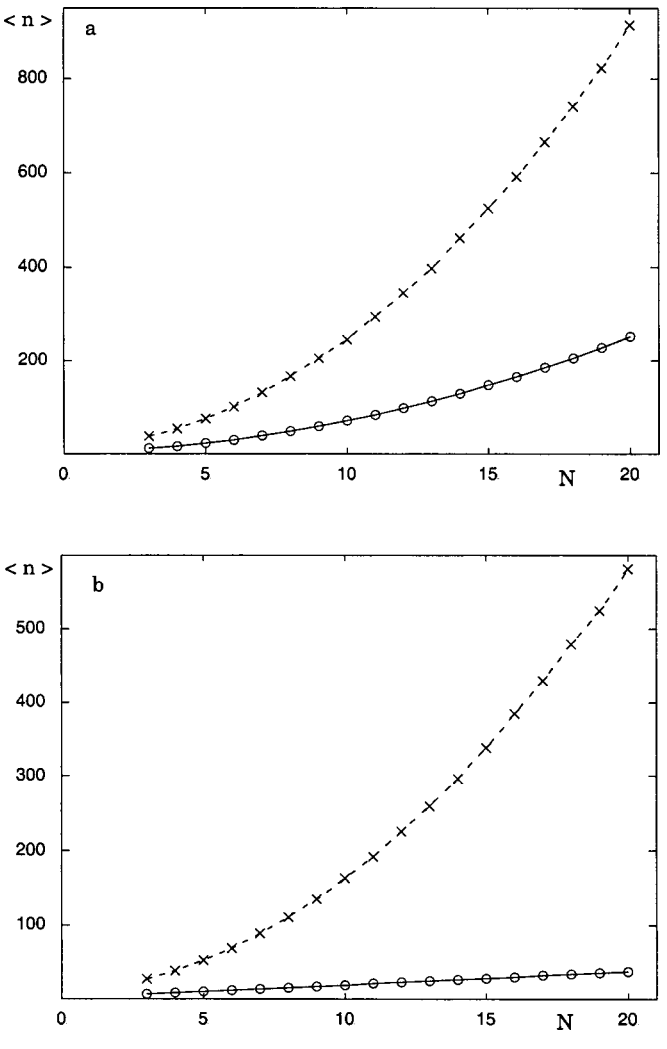

FIG. 3. Mean walk length in the case of the scenarios ($H1L1$) (empty circles) and ($H2L2$) (crosses) and in the presence of extreme Coulomb bias, with no gravity (a) and with finite gravity bias (b).

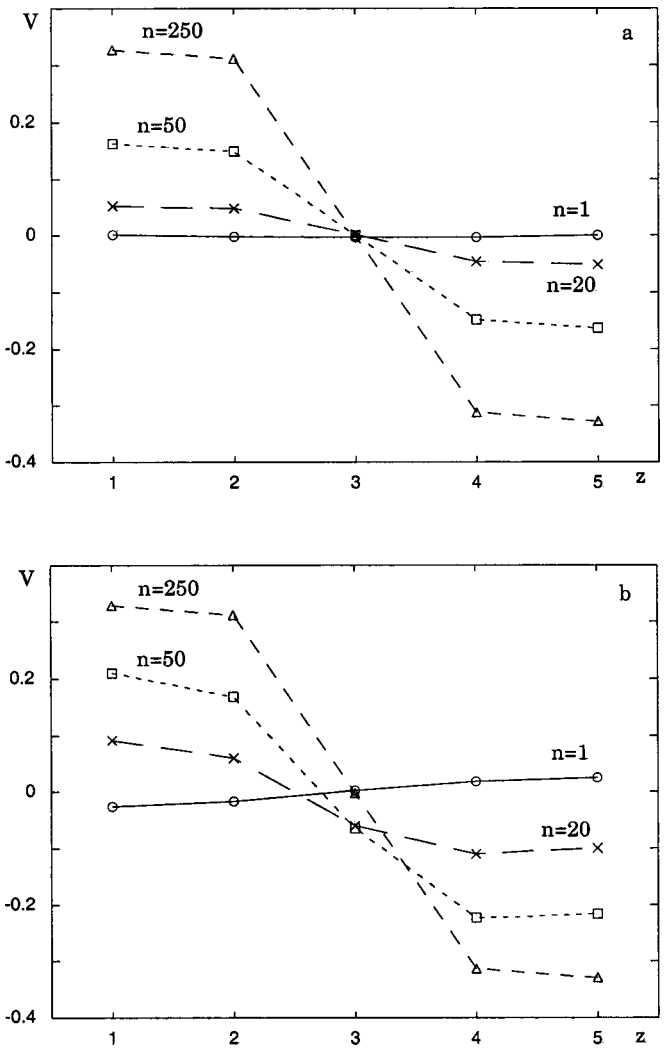

FIG. 4. Electric potential vs vertical distance z at increasing times as obtained from Monte Carlo simulations in a 5×5 lattice in the presence of the Coulomb bias equal to $\frac{3}{8}$ with no gravity (a) and gravity bias equal to $\frac{3}{8}$ (b). The number of realizations is 10^5 and initially the particles are uncharged.

a few kilometers and considerably less in the horizontal direction.

The main result on mean walk length for the scenario ($H1L1$) is summarized in Figs. 1(a) and 1(b) pertaining, respectively, to zero (a) or to finite gravitational bias for the heavy particles (b) after an averaging over 10^5 realizations. Furthermore, in each figure, the cases of no Coulomb bias (empty circles) and of extreme Coulomb bias (crosses) are depicted. As can be seen the dependence of $\langle n\rangle$ with linear size is markedly nonlinear in the absence of gravitation, and tends to become linear when the gravitational bias is increased. One may also notice that the values of $\langle n\rangle$ are well below the upper limit introduced in the beginning of Sec. II.

Figures 2(a) and 2(b) depict the corresponding results for the scenario ($H2L2$). Here, as well as in the sequel H, L are allowed to perform a random walk in the horizontal direction on the boundaries. As can be seen, for the same gravitational bias as before, the dependence of $\langle n\rangle$ with size is now clearly nonlinear. Finally, Figs. 3(a) and 3(b) illustrate the increase of $\langle n\rangle$ in the case of sticky (crosses) versus exit boundary conditions (empty circles) for extreme Coulomb bias and for, successively, zero (a) and finite (b) gravitational bias. Part of this increase arises from the fact that a particle stuck in one of the boundaries can still interact with the second particle in the bulk, thereby delaying its eventual trapping at the other boundary.

As mentioned in the Introduction, quantities such as the mean walk length $\langle n\rangle$ provide relevant information for the purpose of prediction, since they give an estimate, from the first principles, of the characteristic time for electrification. This constitutes, in turn, a lower bound for an electric discharge to occur. In previous work by the present authors [8,9], it was shown that the encounter times are subjected to high variability around their mean. In the present context, this feature reflects the difficulties inherent in issuing quantitative predictions on the time of occurrence of a discharge. It will be addressed in the following section using quantities of more direct relevance than $\langle n\rangle$ itself, such as electric potential differences and electric fields.

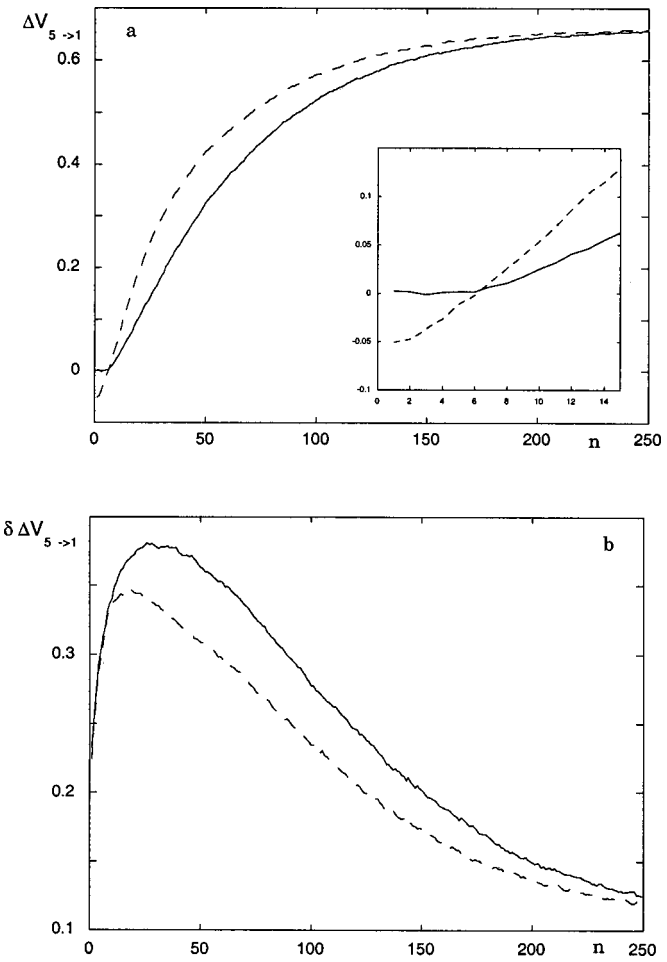

FIG. 5. Mean potential difference (a) and mean square deviation of potential difference (b) without gravity bias (full line) and with gravity (dashed line). Parameters as in Fig. 4.

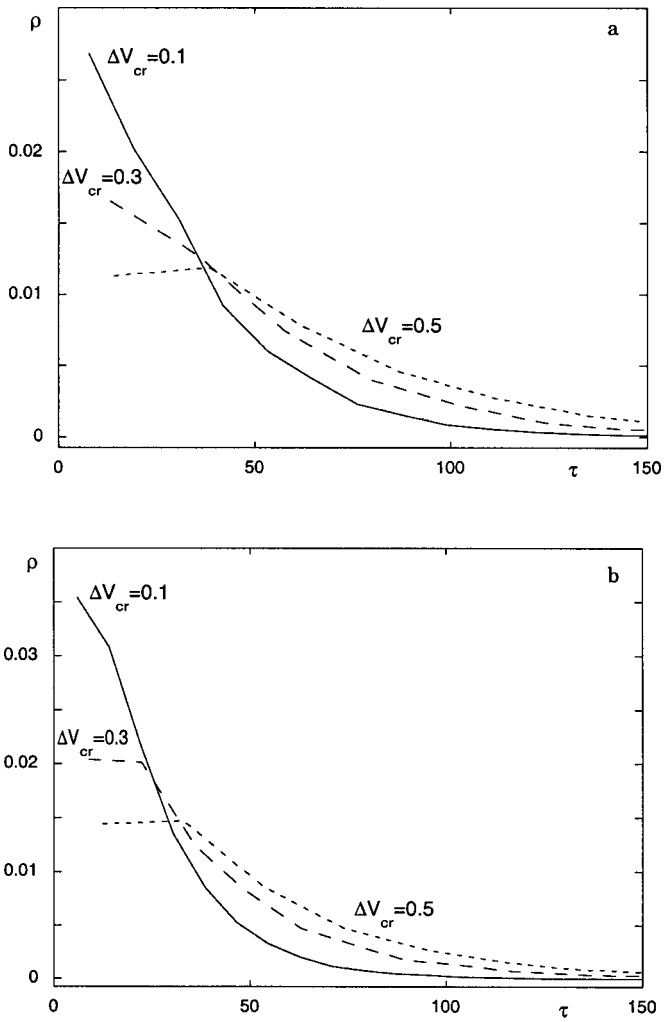

FIG. 6. Probability density of times for the system to reach a prescribed critical potential difference ΔV_{cr} with no gravity (a) and with gravity (b). Parameter values as in Fig. 4.

IV. KINETICS OF ELECTRIFICATION

The Markov and Monte Carlo techniques can be used to monitor the instantaneous positions of the heavy and light particles in their charged configurations and, through them, compute various quantities pertaining to the electrification and discharge processes such as the instantaneous value of local electric potential, electric field, and electrostatic energy within the lattice.

Let $\mathbf{r}$ be the two-dimensional position vector in the lattice, $\mathbf{r}=(i,\ j)$ where i and j run, respectively, over the horizontal and vertical directions. We denote by $\mathbf{r}_{\pm}(t)$ the instantaneous positions of the positively and negatively charged species. The instantaneous electric potential at a point $\mathbf{r}$ in the lattice and the total instantaneous electrostatic energy of the lattice are then (up to a constant multiplicative factor) given by

$$V(\mathbf{r},t)=\sum_{\mathbf{r}'}\frac{\delta^{\mathrm{kr}}_{\mathbf{r}',\mathbf{r}_+(t)}-\delta^{\mathrm{kr}}_{\mathbf{r}',\mathbf{r}_-(t)}}{|\mathbf{r}-\mathbf{r}'|}, \tag{6}$$

$$W(t)=\sum_{\mathbf{r},\mathbf{r}'}\frac{\delta^{\mathrm{kr}}_{\mathbf{r},\mathbf{r}_+(t)}\delta^{\mathrm{kr}}_{\mathbf{r}',\mathbf{r}_-(t)}}{|\mathbf{r}_+(t)-\mathbf{r}_-(t)|}, \tag{7}$$

being understood that $V=0$, $W=0$ when the particles happen to be in their neutral form. As for the instantaneous electric field at point $\mathbf{r}$, it can be computed from Eq. (6) through the discretized version of the relation $\mathbf{E}=-\boldsymbol{\nabla}V$.

For the prototypical model of two reacting and diffusing particles considered in the present work, V and $\mathbf{E}$ would fluctuate in both space and time and W would fluctuate in time in any given realization of the process. Some general trends concerning their behavior can, however, be obtained by averaging expressions (6) and (7) and related quantities over different realizations, each of these realizations being carried out till its termination. In the scenario $(H1L1)$ this means that $\mathbf{r}_{\pm}(t)$ will sooner or later be found outside the lattice: V, $\mathbf{E}$, and W will eventually tend to zero, and after a transient stage of electrification the lattice will be discharged. In contrast, in the scenario $(H2L2)$ the lattice will finally be subjected to charge separation and behave as a condenser, at least until the conditions for a dielectric breakthrough are met. In both cases, the variability of the relevant quantities around the mean will also be probed by constructing appropriate probability distributions.

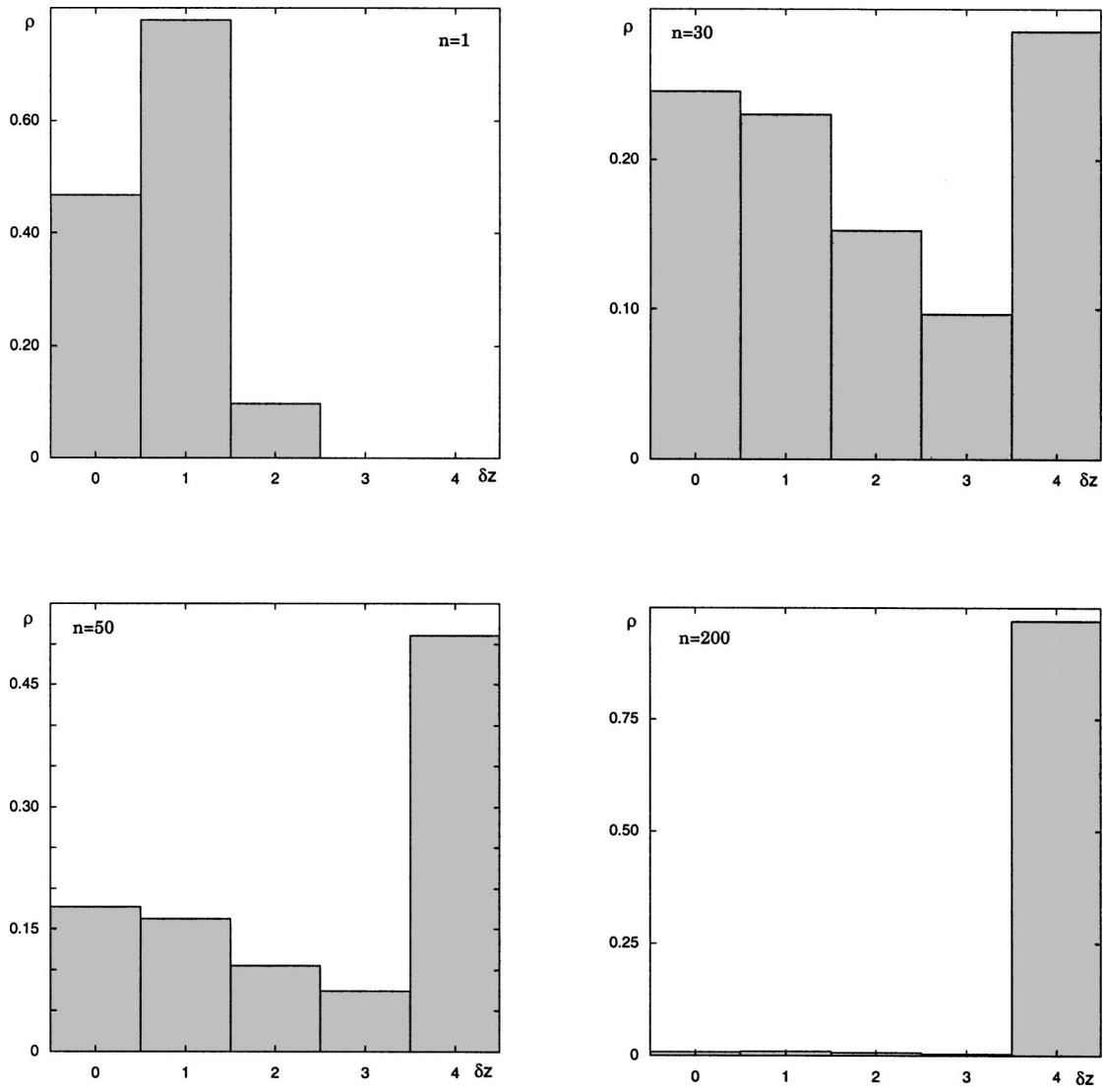

FIG. 7. Probability distribution of the vertical distances of electrified particles at different times under the conditions of Fig. 4(b) and 50 000 realizations.

Figures 4(a) and 4(b) describe the instantaneous mean vertical spatial profiles of the electric potential in a 5×5 lattice in the absence (a) and presence (b) of gravitational bias and for the Coulomb bias equal to $\frac{3}{8}$, in the scenario $(H2L2)$. Figure 5(a) shows how the mean potential difference $\Delta V_{5\rightarrow1}$ between the top and bottom of the layer is building up in the course of time. The standard deviation of the instantaneous potential differences associated with different realizations around this mean is depicted in Fig. 5(b). One observes a high variability of potential differences, close to 50% at the time of the peak value of the mean.

A quantity of great interest that can be inferred from Fig. 5(a) is the time t_{cr} at which a threshold value ΔV_{cr} of the potential difference is crossed. This will provide information on when a discharge can take place by taking appropriate threshold values ΔV_{cr}, as long as these values do not exceed the maximum value that can actually be attained. As an example, for $\Delta V_{\mathrm{cr}}=0.5$ one finds from Fig. 5 in the presence of gravitational bias a time t_{cr} of about 70 units. On the other hand, on the basis of Fig. 5(b) one expects that this value will be subjected to variability. More generally, level crossing processes and extreme value related properties are known to exhibit in their own right a high variability around the mean [11]. To assess the presence of such a property in the problem at hand we monitor the crossing times of the threshold value by the individual realizations of the process, and construct from these data the corresponding probability density. The result is shown in Figs. 6(a) and 6(b) for different threshold values ΔV_{cr} in the absence (a) and presence (b) of the gravitational bias and for a Coulomb bias of $\frac{3}{8}$. We observe the presence of long tails, suggesting that large deviations from the mean can occur with high probability. For the example of $\Delta V_{\mathrm{cr}}=0.5$ considered in connection with Fig. 5, one obtains $\langle t_{\mathrm{cr}}\rangle\approx45.5$, very different from the value $t_{\mathrm{cr}}\approx70$ inferred from the kinetics of the mean potential difference. This reflects the high variability of the process as witnessed also by a standard deviation $\langle\delta t_{\mathrm{cr}}^2\rangle^{1/2}\approx27.1$, quite comparable to the mean. It provides an interpretation of the observation that the times at which an electric discharge occurs are widely distributed and hence difficult to predict. It

also shows that the intrinsic fluctuations generated by the dynamical processes present tend to *advance* the crossing process.

We turn now to a closer analysis of spatial variability. Such variability, if present, would reflect the fact that fluctuations are not manifested coherently at the level of the whole system but possess, rather, a markedly inhomogeneous character. This is supported by recent results showing that inhomogeneous fluctuations tend to be favored when nonlinear dynamical processes are taking place in low-dimensional spaces [12].

An interesting quantifier of spatial fluctuations is provided by Fig. 7, in which the histogram of the vertical distances $|z_+ - z_-|$ of the charged particles in a 5×5 lattice recorded in the different realizations of the process is constructed for the scenario $(H2L2)$ and in the presence of the gravity and Coulomb bias equal to $\frac{3}{8}$. We see that prior to its settling to a value equal to the vertical size of the cloud, this variable exhibits strong fluctuations. These are manifested by a ''seeding'' process where, starting from a homogeneous situation, large distances become suddenly realized at about 30 time units. Following this seminal event a substantial probability mass is built in the range of these distances, such that at about 50 time units (a time of the order of the mean encounter times computed in Sec. III) one observes a transient bimodality.

The above behavior has interesting repercussions in the properties of the local electric field. To derive these properties the instantaneous values of the field are recorded in each lattice point. From this information, their mean $\overline{E}$, maximum $E_{\max}$, and minimum $E_{\min}$ over the lattice are deduced at each time. Carrying the process for different realizations one can then construct the statistical properties of these quantities. Figure 8 depicts the time dependence of $\langle\overline{E}\rangle$, $\langle E_{\max}\rangle$, $\langle E_{\min}\rangle$ and of the associated standard deviations over the realizations for a 5×5 lattice. As can be seen, the local electric field varies over a wide range of values while its spatial mean remains very small for all times. This is further illustrated in the histograms associated with these quantities shown in Fig. 9 at a time of $n=50$ of the order of the mean encounter time (Table I). The most probable value of $E_{\max}$ is about 0.15, which is just what one obtains by dividing the plateau value of $\Delta V_{5\to1}$ in Fig. 5(a) by the vertical size of the lattice. But as the figure shows, much higher values of $E_{\max}$ can also be sustained in the lattice and persist for long times. Such ''hot spots'' are natural candidates for initiating a microdischarge. The latter will die out or evolve to a full-fledged lightning according to whether the heat and charge transfer rates will be faster or slower than the time scale of the local (reactive) dynamics. This could provide a rationale of recent observations [13] that the conventional breakdown mechanism alone cannot trigger lightning. This view is further corroborated by the time dependence of the electrostatic energy [Eq. (7)], shown in Figs. 10(a) and 10(b) in cases $(H1L1)$ (a) and $(H2L2)$ (b). In both cases the particles are initially taken to be in the uncharged configuration. We see that the energy first evolves toward a maximum that is reached at a time close to the value given in Table I under the relevant conditions. Subsequently, it falls off on a longer time scale reaching a value equal to zero in case $(H1L1)$ and to a finite plateau in case $(H2L2)$. In a one-dimensional

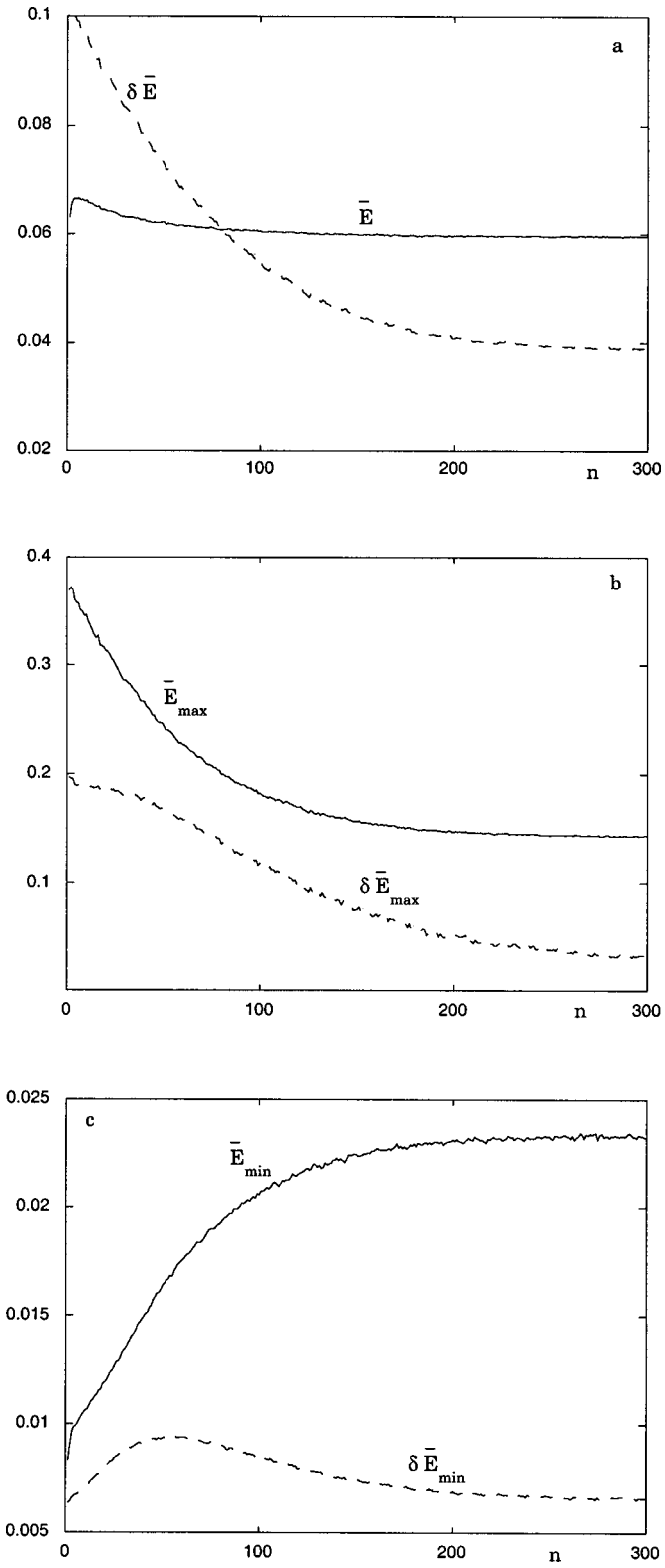

FIG. 8. Time evolution of the mean (full lines) and mean square deviation (dashed lines) of the electric field (a), and its local extreme values, maximum (b) and minimum (c). Number of realizations is 50 000 and parameter values as in Fig. 4(b).

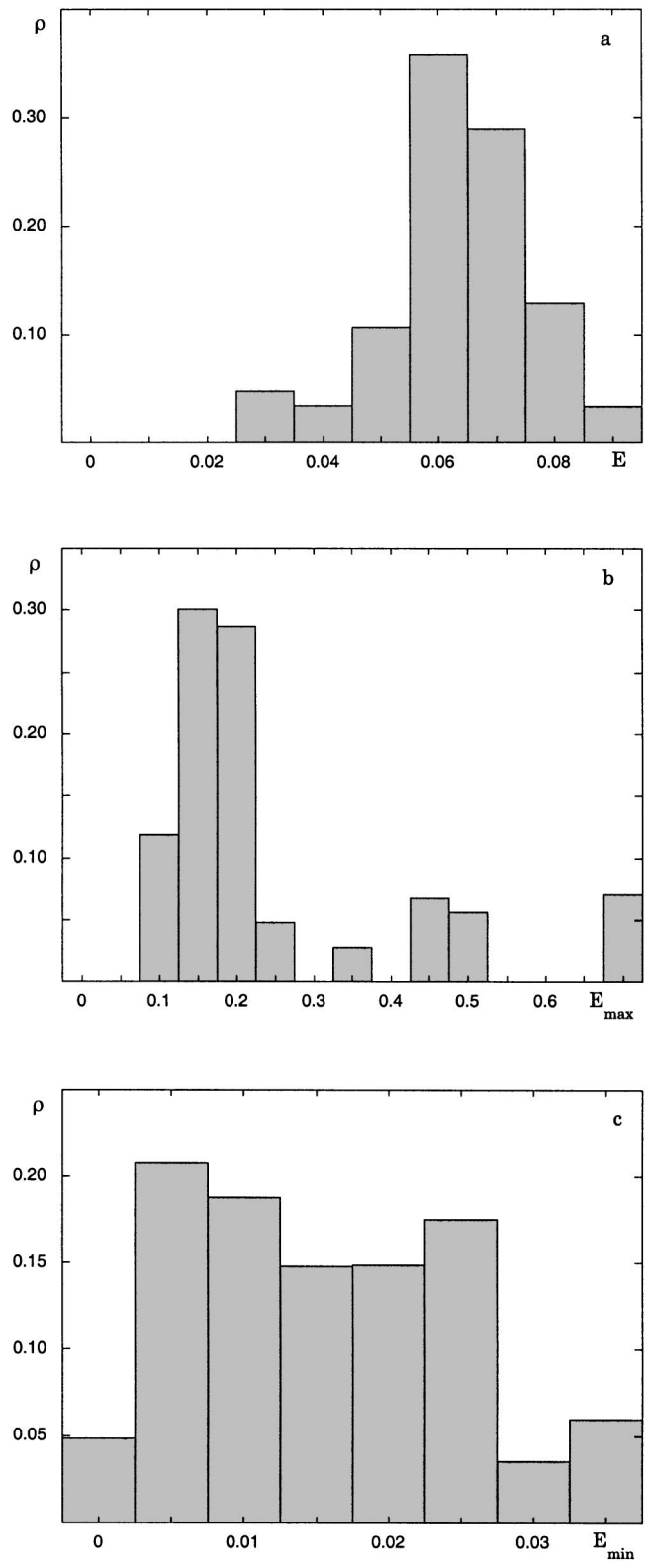

FIG. 9. Probability density of the quantities of Fig. 8(a)–(c) at $n=50$.

system, the value of the latter would be just 0.25 (the inverse of the height of the lattice) multiplied by the probability (roughly equal to $\frac{1}{2}$) that the particles reach the boundaries in their charged configurations. In the present case of the two-

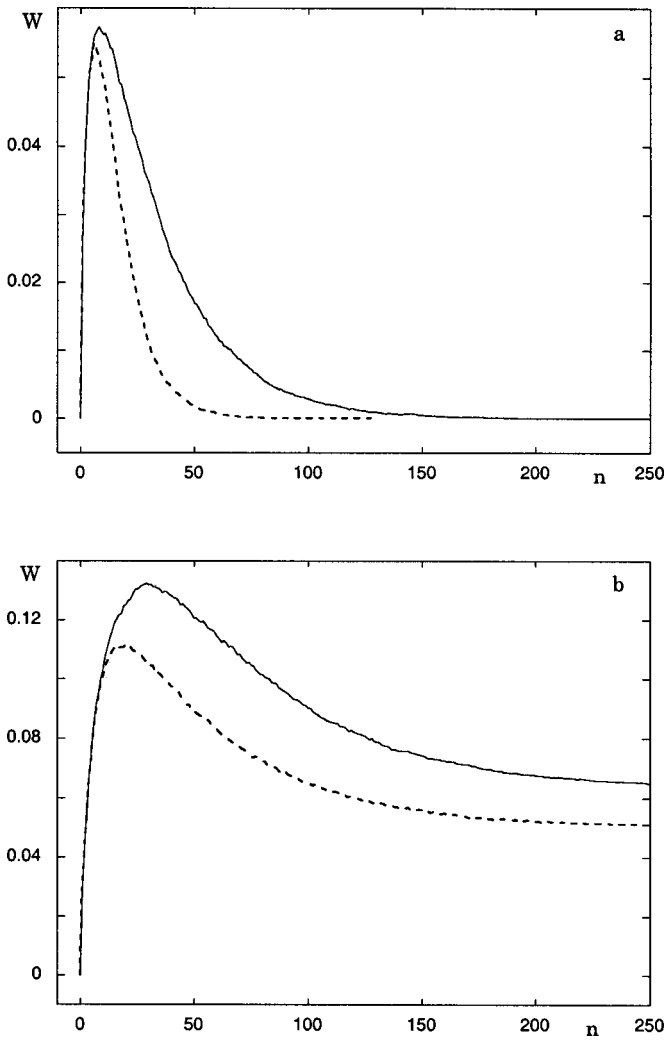

FIG. 10. Time dependence of the electrostatic energy $W(t)$ in a 5×5 lattice averaged over 10^5 realizations in cases $(H1L1)$ (a) and $(H2L2)$ (b) for zero gravity (full line) and for gravity bias (dotted line) equal to $\frac{3}{8}$. Coulombic bias is set to $\frac{3}{8}$ and initial conditions correspond to neutral particles.

dimensional lattice the value is smaller, since the particles are allowed to move in the horizontal direction as well.

V. CONCLUSIONS

The study of electrical structure in thunderstorm clouds has proved to be an ongoing source of fascination and frustration for generations of meteorologists. Recent reviews [2,3] stress the need for both further laboratory investigations of charge transfer and modeling studies of charge separation in the presence of gravity and convection.

The study undertaken in the present paper reveals the rather remarkable fact that even when the complex, synergetic processes of charge formation or neutralization, diffusion and gravitational bias are stripped down to design the simplest possible lattice-statistical model, one arrives at a qualitative understanding of the onset of spontaneous electrification. Furthermore, a number of subtle effects are already at play at that level of description leading to the onset (or

not) of nonlinear behavior in the lifetime of the system as a function of spatial extent, to high spatiotemporal variability and to nontrivial kinetics.

Consider first Fig. 1. In the scenario $(H1L1)$, wherein heavy and light particles survive until one or the other exits the system, the profile of the system lifetime (as monitored by the mean number of particle displacements before termination) as a function of the system size displays a distinctly nonlinear character in the absence of a gravitational bias on the motion of the heavy particle. However, upon introducing a gravitational bias (by imposing an enhanced probability that the heavy particle moves vertically downward and a correspondingly smaller probability that it moves vertically upward), both the qualitative and quantitative behaviors of the evolution profile change. Qualitatively, the nonlinear behavior evident in Fig. 1(a) collapses to a quasilinear behavior in Fig. 1(b). And, quantitatively, there is more than a sixfold decrease in the lifetime of the system when a gravitational bias influences the random, diffusive motion of the heavy particle.

In the scenario $(H2L2)$ wherein the heavy particle is entrained on the lower boundary and the light particle on the upper boundary on first encounter, whereas the evolution profiles in the absence [Fig. 2(a)] and presence [Fig. 2(b)] of gravity are both nonlinear, there is now a remarkable dilation in the time scale of the process *vis-à-vis* the scenario $(H1L1)$, viz., a fourfold increase in the absence of gravity and a 12-fold increase in the presence of gravity. These qualitative differences are shown plainly in Fig. 3.

Also evident in Figs. 1–3 is the relative unimportance of the Coulomb bias, even taken in the extreme limit wherein neutralization occurs with unit probability when the two charged species, in their otherwise random motion, happen to occupy nearest-neighbor sites on the lattice. The qualitative effect of introducing the Coulomb bias is to dilate slightly the lifetime of the process, this owing simply to the time delay induced by the neutralization step.

An important feature that came out from the subsequent analysis is the high temporal and spatial variability of the process and its repercussions in the electrification and discharge processes. In particular, the pronounced dispersion of the time at which the system may cross a threshold value of potential difference (Fig. 6) and the fact that high electric field values can occur transiently with appreciable probability (Fig. 9) suggest a nucleation-type mechanism, whereby microdischarges are initiated around hot spots within the lattice. They also draw attention on the need that the monitoring and prediction methods of discharges in real clouds should integrate the high dispersion of impact times and impact points, inherent in such a spatiotemporal variability.

Much of the analysis of the two-particle system carried out in this work can be applied to the more realistic case of a dilute many-particle system, in which the mean time between successive binary collisions is longer than the exit time of one of the particles of a colliding pair. The only new effect would be a density-related one, causing an increase of the time of the overall termination of the process owing to the availability of more than one colliding pairs. Of more interest would be to incorporate many-body effects in the Monte Carlo and the Markovian analysis giving rise, in particular, to particles participating in repeated binary collisions or ternary and higher-order ones. The electrification process would undoubtedly become more intricate. In particular, it could yield the multipolar structure known to occur in real world clouds [2,3], instead of the dipolar structure characteristic of our two-particle system.

ACKNOWLEDGMENTS

This work was supported by a NATO Cooperative linkage Grant No. PST.CLG.977780 and by the Belgian Federal Office for Scientific, Technical and Cultural Affairs under Contract No. MO/34/004.

[1] D. Mackeras and M. Darveniza, J. Geophys. Res. **99**, 10 813 (1994).

[2] R. A. House, Jr., *Cloud Dynamics* (Academic, New York, 1993); H. R. Pruppacker and J. D. Klett, *Microphysics of Clouds and Precipitation* (Kluwer Academic, Dordrecht, 2000).

[3] M. Stolzenburg, W. D. Rust, and T. C. Marshall, J. Geophys. Res. **103**, 14 097 (1998).

[4] S. Vannitsem, *Aspects Statistiques et Dynamiques de l'Activité Orageuse Mesurée par SAFIR sur la Belgique*, Scientific and Technical Publication Number 014 (Royal Meteorological Institute of Belgium, Brussels, 2000).

[5] R. Houze, *Cloud Dynamics* (Academic, San Diego, 1993).

[6] L. Matteev, *Physics of the Atmosphere* (Israel Program for Scientific Translations, Jerusalem, 1967).

[7] R. Rogers, *A Short Course in Cloud Physics* (Pergamon, Oxford, 1979).

[8] J. J. Kozak, C. Nicolis, and G. Nicolis, J. Chem. Phys. **113**, 8168 (2000).

[9] C. Nicolis, J. J. Kozak, and G. Nicolis, J. Chem. Phys. **115**, 663 (2001).

[10] J. J. Kozak, Adv. Chem. Phys. **115**, 245 (2000); G. H. Weiss, *Aspects and Applications of the Random Walk* (North-Holland, Amsterdam, 1994).

[11] G. Nicolis, V. Balakrishnan, and C. Nicolis, Phys. Rev. E **65**, 051109 (2002).

[12] R. Kopelman, Science (Washington, DC, U.S.) **241**, 1620 (1988); A. Ovchinnikov and Yu. Zeldovich, Chem. Phys. **28**, 215 (1978).

[13] R. Solomon, V. Schroeder, and M. Bakar, Q. J. R. Meteorol. Soc. **127**, 2683 (2001).